Prabha Materials Science Letters
Vol. 5, No. 2, 272-285, 2026
https://doi.org/10.33889/PMSL.2026.5.2.015

Temperature-Dependent Self-Diffusion Behaviour of Copper: A Molecular Dynamics Study

Harendra Singh Bohara
Department of Physics,
Radhey Hari Government Post Graduate College, Kumaun University, Nainital, Uttarakhand, India.
E-mail: hsbohara14@gmail.com

Riya Gola
Department of Physics,
Radhey Hari Government Post Graduate College, Kumaun University, Nainital, Uttarakhand, India.
E-mail: riyagolaksp@gmail.com

Mahipal Singh
Department of Physics,
Radhey Hari Government Post Graduate College, Kumaun University, Nainital, Uttarakhand, India.
E-mail:dmpsc@rediffmail.com

S. K. Joshi
Department of Applied Science,
Shivalik College of Engineering, 248007, Dehradun, Uttarakhand, India.
Corresponding author: mail.skj@gmail.com

(Received on December 28, 2025; Revised on May 12, 2026; Accepted on May 15, 2026)

Abstract
Understanding the kinetic properties of copper (Cu) becomes very important, where the atomic migration directly impacts the mechanical and electrical reliability of the product. In the present work, the effect of temperature on the diffusivity of copper is analysed using the Molecular Dynamics (MD) simulation technique, which has emerged as an effective alternative to experimental methods, especially when carrying out experiments becomes challenging. Large-scale Atomic/Molecular Massively Parallel Simulator (LAMMPS) is employed to simulate the experimental diffusion pattern in copper at three selected temperatures. The Simulations are performed with the help of Embedded Atom Method (EAM) pair potentials and Periodic boundary conditions, which are applied to reduce edge effects and replicate the behaviour of copper atoms. For the modelled system, the mean squared displacement (MSD) of the particles is used to estimate the diffusion coefficient, which showed a good agreement with the experimental data reported in the literature. The analysis of the radial distribution function also indicates that the modelled system retained its structural integrity without premature melting at the selected temperature values. These results may prove to be very significant for understanding the phase transformations, mechanical properties, and alloy design with copper.

Keywords- Embedded atom method, LAMMPS, Diffusion, Mean squared displacement, Molecular dynamic simulation.

1. Introduction

Copper (Cu) is a transition metal that crystallizes in a face-centred cubic structure with a lattice constant of 0.3615 nm (Li et al., 2016; Trong et al., 2022). Copper has unique malleability and ductility. It possesses exceptionally high thermal and electrical conductivity. Owing to these properties, copper and its alloys have become highly useful in the aviation, manufacturing, and electronics industry (Li et al., 2014). In addition to its remarkable heat conductivity, copper metal exhibits good mechanical characteristics (Zhang et al., 2024), and its alloys are vital in science and technology. Due to its distinctive features and prospective uses across various areas, copper metal has garnered considerable interest over the last 20 years. For example,

non-agglomerated, spherical, homogeneous copper nanoparticles are required for conductive films and nanofluids (Kart et al., 2014). Copper also demonstrates favorable mechanical behaviour, making it a notable commercial material for applications where diffusion processes significantly influence its performance. Diffusion in metals and their alloys plays a vital role in determining their mechanical and electrical characteristics. For example, Surface alloying and compositional changes at the interface caused by direct diffusion may result in major modifications to mechanical and electrical parameters (Butrymowicz et al., 1973). The diffusion coefficient that comprises tracer, mutual, chemical, self, transport, collective, and intrinsic diffusion coefficients is the most significant indicator of diffusion (Zhang et al., 2023). Self-diffusion represents the fundamental mechanism of atomic mobility in crystalline solids and is facilitated by existing point defects such as vacancies and interstitials (Posselt et al., 2022). It strongly correlates with local structural and thermodynamic properties, as well as interatomic interactions (Li et al., 2024). Understanding self-diffusion is essential for simulating microstructural evolution, including recovery, creep, and grain boundary motion, especially during alloy formation (Hargather & O'Connell, 2022). The determination of the self-diffusion coefficient of copper at three temperatures, 715 K, 836K, and 905 K, has both scientific and practical significance, as vacancy-induced atomic motion becomes prominent at these temperatures, enabling an accurate estimation of diffusion coefficients. Further, the precise self-diffusion data is crucial for the prediction of the long-term stability of copper and alloys used in wiring, thermal devices, and electronic interconnects operating at high temperatures. Such information is also important for improving technologies aimed at designing materials with optimized structural and functional parameters (Talanin & Talanin, 2016). Historically, several experimental studies have been done to calculate the diffusion coefficients of copper.

Maier (1977) determined the self-diffusion coefficient of copper, over a temperature range of 359 to 632°C, utilizing radioactive tracers with the serial sectioning technique. Kuper et al. (1954) employed tracer methods combined with precision grinding and lathe tools to measure diffusion between 685 and 1062 °C. Rothman & Peterson (1969) used radiotracer techniques to study the diffusion of Cu^{64} and Cu^{67} in single-crystal copper at temperatures between 890 and 1060 °C. Steigman et al. (1939) further extended such measurements using radioactive isotopes between 750 and 950 °C. However, these experimental methods are time-intensive and require sophisticated, expensive instrumentation along with the user's expertise. These limitations can be addressed by the molecular dynamics (MD) simulation method, which has proven itself as an efficient computational tool for studying atomic-scale diffusion mechanisms in metals and alloys (Tatsumi et al., 2023) in different temperature ranges. MD was developed in the 1950s and has provided researchers with microscopic insights into particle interactions and accurately predicted material properties related to structure and thermodynamics (Chui et al., 2015; Kart et al., 2014). Atomistic simulations using appropriate interatomic potentials can significantly enhance our understanding of diffusion processes and provide reliable predictions at considerably reduced cost and computational time (Barbhuiya & Das, 2023; Yin et al., 2024). It has been demonstrated that molecular dynamics simulation provides numerous benefits in comprehending the diffusion mechanisms at the microscopic level and illustrating the evolution of the atomic-scale structure (Yang et al., 2019).

In the present work, the MD simulation technique has been applied to estimate the self-diffusion coefficient of copper at the above-mentioned temperatures. These studied temperatures are strong enough to demonstrating a continuous monotonic behaviour. The Mean Squared Displacement (MSD), Radial Distribution Function (RDF), and microstructure analysis have been used to understand the diffusion behaviour in copper comprehensively. The self-diffusion coefficients obtained via the present computational approach have been compared with the available experimental data for validation. The values of self-diffusion coefficients estimated via the present framework are closely consistent with the reported experimental results and show a similar trend. The visualization formalism adopted will help researchers to

understand the diffusion-related phenomena more clearly. Additionally, the present method offers a reliable approach for estimating the diffusion-related parameters of copper and its alloys.

2. Methodology and Simulation Details

In the present work, a MD simulation approach has been applied to calculate the self-diffusion coefficient of copper at the specified temperatures. A small cubic simulation box with dimensions of $36.15A^0x36.15A^0x36.15A^0$ has been created by replication of the conventional FCC unit cell of copper 10x10 x10 times with a lattice constant of 3.615 A^0, comprising 4000 copper atoms (**Figure 1)**, which are located on optimal lattice sites indicating bulk copper. This methodology gives an atomic density that is in agreement with the bulk density of copper reported in experiments. Periodic boundary conditions are used in all directions, X, Y, and Z to remove the surface effects.

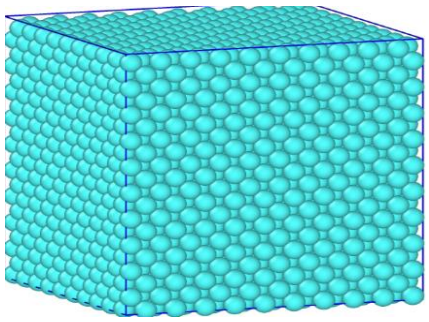

Figure 1. Simulation box with 4000 copper atoms.

The Large-scale Atomic/Molecular Massively Parallel Simulator (LAMMPS), a programme, written in C^{++}, is used to execute all simulations in the copper system (Mao et al., 2020; Ye et al., 2025). To properly define atomic interactions, the atomic structure must be developed, and a proper interatomic potential should be assigned via a LAMMPS input script. An input script is a carefully developed code describing every important element necessary to start, run, and evaluate the simulation findings. Setting the essential simulation parameters, which include units, dimensionality, atom type, and periodic boundary conditions, is the initial step in the process. **Table 1** describes the input script parameters used in the present study.

Table 1. Summary of input script parameters used in MD simulation.

S. No.	Parameter	Value used	Description
1.	Units	metal	unit system: A^0, ps, eV, K,ns
2.	Element	Copper	metal simulated
3.	Crystal Structure	-	Face-Centred Cubic (FCC)
4.	Lattice Parameter	3.615 A^0	For Cu
5.	Supercell size	10 x 10 x 10	FCC unit cells
6.	Density	8.96 gm/ cm^3	FCC Cu
7.	Total number of atoms	4000	Number of atoms simulated
8.	Pair-Potential	eam/alloy	Interatomic potential for copper
9.	Boundary condition	-	Periodic boundary in X, Y, AND Z direction
10.	Box Dimension	36.15 A^0 X 36.15 A^0 X 36.15 A^0	Box Size 36.15 A^0 in each Direction
11.	Temperature	715K, 836K, 905K	Temperatures at which diffusion coefficient calculated
12.	Ensemble	NVT	Canonical ensemble
13.	Thermostat		Nose-Hoover (To control temperature)
14.	Thermostat Damping	100 fs	Controlling temperature response
15.	Output sampling interval	100 steps	Frequency of data recording
16.	Timestep	1 fs	Time step for integration
17.	Run	50ps. 5ns	Equilibration and production run

To define the interactions between atoms, the Embedded Atom Method (EAM) potentials for copper, developed by Mishin et al. (2001), have been used. In the Embedded atom method, an atom's energy depends on its location and local electron density. The total energy is determined by the Equation (1)

$$E_a = \frac{1}{2}\sum_{a.b(a\neq b)} \emptyset_{ab}(r_{ab}) + \sum_i F_{ab}(\overline{\rho}_a) \quad (1)$$

where, E_a is the total energy of N atoms, r_{ab} is the distance between atoms *a* and *b*, F_{ab} is the embedding energy function of the electron density, $\overline{\rho}_a$ is the electron density at atom *a* contributed from atom *b*, and $\emptyset_{ab}(r_{ab})$ is the short-range pair potential function (Yang et al., 2011). Where $\overline{(\rho}_a)$ is given by Equation (2)

$$\left(\overline{\rho}_a\right) = \sum_{b\neq a} f(r_{ab}) \quad (2)$$

In the present formulation of total energy, the functional form $F_{ab}\left(\overline{\rho}_a\right)$, $\emptyset_{ab}(r_{ab})$, and $f(r_{ab})$ are related to Mishin-type parameterization (Mishin et al., 2001). which provides a well-fitted description of the diffusion behaviour of metals and alloys at different temperature ranges.

Before the start of the final simulation run, the model system computational box is first stabilized by applying energy minimization and then equilibrated. The evolution of the simulated sample is regulated by thermodynamic and ensemble variables, which include integration settings, temperature, and volume control. Before compiling any data, the system is equilibrated using the NVT ensemble with a Nosé–Hoover thermostat for 50 picoseconds. The equilibration of the system before any production run allows the atoms to adjust their natural distributions of velocities and positions. It conserves the system's total energy and permits the atoms to evolve automatically according to their atomic interactions. After equilibrating the system, a simulation is carried out for 5 nanoseconds under the same NVT ensemble to determine the Mean Squared Displacement (MSD) values of the copper at the above-mentioned temperatures. The MSD can be determined as-

$$\text{MSD} = \langle |r(t) - r(0)|^2 \rangle = \frac{1}{N}\sum_{b=1}^{N} < |r_b(t) - r_b(0)|^2 > \quad (3)$$

where, *N* denotes the total number of atoms, and $r_b(t)$ and $r_b(0)$ are the position vectors of atom *b* at times *t* and 0, respectively. The value of the self-diffusion coefficient of the copper can be calculated by the slope of the fit curve of MSD vs. time. It provides an efficient and reliable approach for the exact calculation of the diffusion coefficient (Riahi et al., 2019). The diffusion coefficient is given by standard Einstein relation as-

$$D = \lim_{t\to\infty} \frac{1}{6Nt}\sum_a^N <|r_b(\mathrm{t}) - r_b(\mathrm{t}_0)|^2 > \quad (4)$$

where, *N* is the number of penetrants, $r_b(t)$ and $r_b(t_0)$ are the beginning and final location of the penetrant's centre of mass over the time interval *t*, and $\langle |r_b(t) - r_b(t_0)|^2 \rangle$ is the average mean square displacement.

The diffusion coefficient obtained by the above relation is in Å^2/ps. It is converted into cm^2/sec according to the relation:

$$1\ \text{Å}^2/\text{ps.} = 10^{-4}\ \text{cm}^2/\text{sec.}$$

To describe the structural characteristics of copper, the radial distribution function, $g(r)$, has been used in the present study. It illustrates the molecular system's structure and defines the change in particle number density with distance from a reference particle (Wade et al., 2018). It describes the configuration of particles in an atomic sample under designated conditions. Additionally, the pattern of this computational quantity

is utilized as a phase indicator for atomic structures (Singh et al., 2025). Its value is given by an Equation (5)

$$g(r) = \frac{1}{4\pi\rho r^2 N} \sum_{i=1}^{N} n_i(r) \quad (5)$$

where, r is the radial distance from a reference point, N is the total number of atoms, ρ is the number density, and $n_i(r)$ is the number of atoms at a distance r from the i^{th} atom. If
$g(r)$ =1, random distribution,
$g(r) \rangle$ 1, higher order of probability of finding atoms at a distance r,
$g(r)$ =0, no atoms is found at a distance r.

Newton's second law of motion is used to calculate the particle's position and velocity by applying the Velocity-Verlet algorithm.

$$F = ma = m\frac{d^2 r}{dt^2} \quad (6)$$

The Velocity-Verlet algorithm updates the position and velocity of atoms according to Equations (7) and (8).

$$r(t + \delta t) = r(t) + \dot{r}(t)\delta(t) + \frac{1}{2}\ddot{r}(t)\delta t^2 \quad (7)$$

$$\dot{r}(t + \delta(t) = \dot{r}(t) + \frac{1}{2}\,[\ddot{r(t)} + \ddot{r}(t + \delta(t)]\delta(t) \quad (8)$$

where, δt is the time steps after which it updates the position and velocity of the atoms.

3. Result and Discussions

3.1 Temperature Dependence of the Total Energy of Copper

Before estimating the parameters like MSD and RDF, the present system is equilibrated for its stability. To analyse the stability the energy/atom vs. time graphs have been plotted at the targeted temperatures (**Figure 2**). The dotted line with each curve represents the average energy values of atoms at each studied temperature (**Table 2**). The present system appears thermodynamically stable during the simulations, as indicated by the small vibrations that solid curves display around their corresponding average-value lines. As the temperature increases, there is a minor rise in the average energy per atom, which may be attributed to the larger atomic vibrations at higher temperatures. This steady pattern indicates that the system is well equilibrated over all temperatures and that enhanced atomic movement and diffusion are associated with increasing average energy. At higher temperatures, a higher average energy indicates that atoms have greater thermal energy for crossing the barriers. We further observe that the average energy becomes less negative with increasing temperature, and there is no large energy shift with increasing temperature. Hence, a gradual increase in the thermal energy with temperature is consistent with enhanced diffusion behaviour.

Table 2. Average energy /atom of copper at different temperature.

S. No.	Temperature(K)	Average energy(ev)
1.	715	-3.437
2.	836	-3.428
3.	905	-3.423

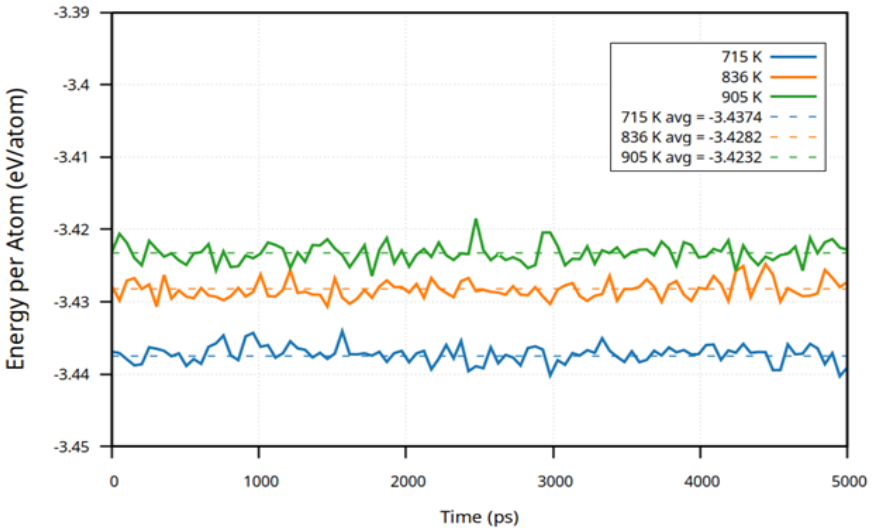

Figure 2. Energy vs. time curve of copper at different temperatures.

3.2 Structural Characterization Using Radial Distribution Function (RDF)

The radial distribution function of copper at three different temperatures (**Figure 3**). The plot of the radial distribution function $g(r)$ at these temperatures allows an in-depth understanding of the temperature-dependent structural behaviour of copper during molecular dynamics simulations. The FCC crystal structure is preserved throughout the examined temperatures, as all three curves show their main peaks at the same characteristic distances. The nearest-neighbour distance, or the most likely spacing between directly bound or closely packed atoms in the lattice, is indicated by the first strong peak in the RDF plot, which is situated at around 2.5 Å. The first coordination shell, where atoms are tightly linked, is indicated by this peak. At each examined temperature, the initial peak retains its sharpness and intensity, but merely broadens and lowers in height as the temperature goes up. This stability demonstrates that short-range order remains strong even at 905 K. Atoms, which are somewhat farther apart but stay inside the crystal's short-range order, are shown by the second peak, which is very close to 3.8 Å and illustrates the second coordination shell. Its position, with only a small amplitude reduction and profile smoothing, shows that mid-range order continues to persist when temperature increases. The longer-range atomic correlations, usually including atoms from the third coordination shell, are represented by the third peak, which is located at about 4.4 Å. It's noteworthy that, irrespective of maximum temperature, the fourth peak, which lies between 5.3 and 5.5 Å, shows no signs of disappearing, indicating that long-range order continues to be maintained. However, as the temperature rises, an apparent decrease in peak height has been noticed. This reduction implies that atomic vibrations amplify at higher temperatures, which decrease the chance of finding nearby atoms at accurate lattice locations. The first peak is conspicuous and vivid at 715 K, suggesting a well-defined nearest-neighbour separation indicative of a highly ordered solid. This peak appears broader and slightly lower at 836 K, showing the atomic position changes due to thermal vibrations. Lattice expansion enables all peaks to slightly relocate to the right as the temperature increases. We have used a vertical offset to achieve visual separation of peaks at the investigated temperatures. The vertical offset added between the curves does not modify the comparative analysis. Overall, the RDF growth reveals that, instead of the collapse of the structure of the present system, the FCC structural framework of copper remains intact up to 905 K, with only small broadening and overlap of the coordination shell. This substantial overlapping of the RDF peaks illustrates that the system preserves its structural integrity even at higher temperatures without drastically affecting lattice order. These RDF attributes are completely in

line with experimental predictions. These simulations' efficiency in detecting temperature-dependent modification in solid copper is therefore verified by the RDF results, which further endorse the simulations' reliability.

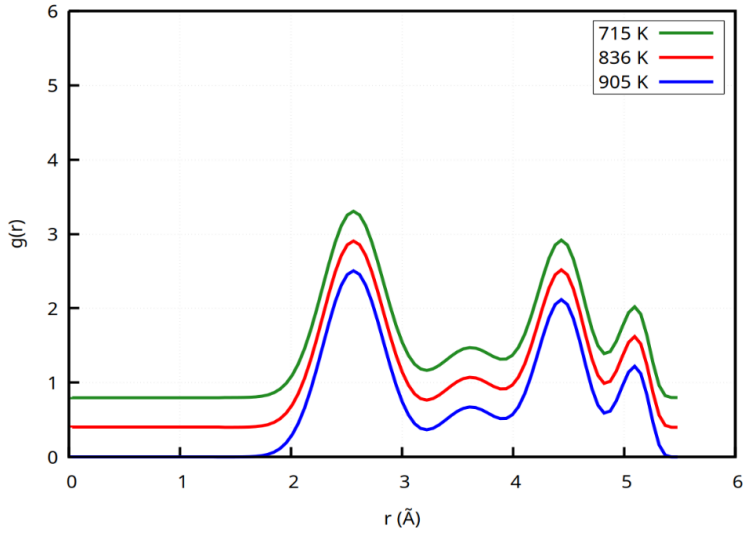

Figure 3. Radial distribution function curve of copper at different temperatures.

3.3 Diffusion Behaviour: Mean Squared Displacement (MSD) Study

To analyse the diffusion behaviour of the present system at 715 K, 836 K, and 905 K, a graph is drawn between the mean-squared displacement and time. The MSD values are computed after thermal equilibrium is achieved. **Figure 4** illustrates the variation in MSD values at the investigated temperatures.

From **Figure 4(a)**, we observe that initially, the MSD vs. time curve of copper at 715 K is almost flat. This flat profile indicates that there is no observable long-range motion, revealing that atoms mainly oscillate about their equilibrium lattice points. At the end points, there is only a slight surge (~4000ps.), which exhibits a small amount of diffusion. This type of behaviour at 715 K is a property of solids much below the point where detectable self-diffusion takes place and suggests that atomic structure remains nearly ordered and stable.

Figure 4(b) illustrates the MSD vs. time curve of copper atoms at 836 K. This curve shows that the MSD value approaches the range of 10^{-5} Å^2, which is greater than that of 715 K. After reaching near 3000 ps., the curve gradually rises, marking thermally initiated atomic hops. The curve exhibits higher fluctuations, which are indicative of irregular displacements facilitated by defects.

Figure 4(c) shows the variation in the MSD with time at 905 K. This curve begins to rise earlier, between 2500 and 3000 ps., and approaches the 10^{-4} Å^2 scale, which is nearly an order of magnitude larger than the 836 K curve. Atoms migrate substantially due to thermal effects at this temperature, which indicates that material is entering a distinct self-diffusion regime.

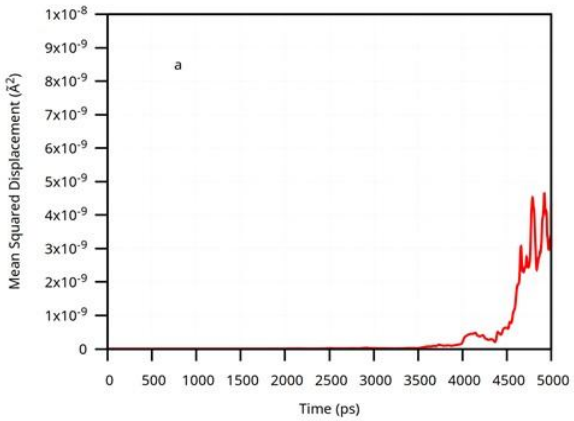

(a) 715 K

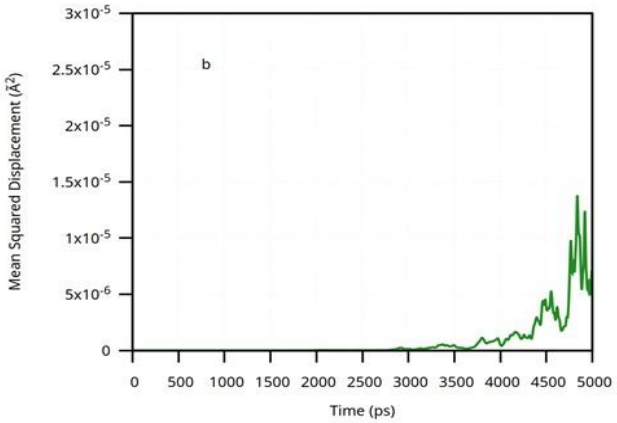

(b) 836 K

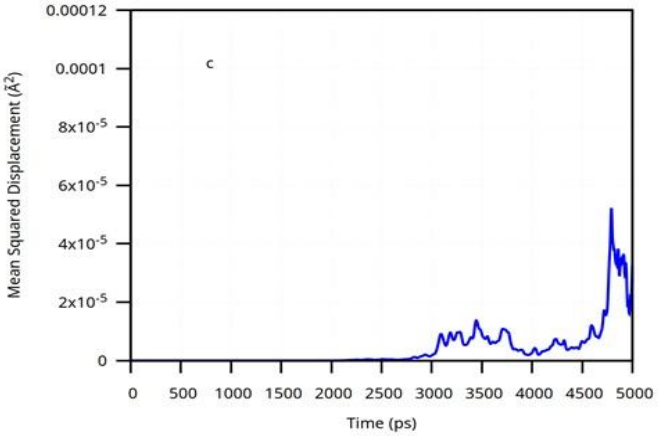

(c) 905 K

Figure 4. Mean squared displacement (MSD) vs time curve for copper metal at three selected temperatures (a) 715K (b) 836K (c) 905K, using MD simulation technique.

Hence, it is established that the MSD curves decisively indicate that atomic movement grows with temperature. Atoms are restricted to vibrational motion within their lattice locations, which can be observed through the MSD curve, appearing almost flat at 715 K. Thermally triggered jumping commences when the MSD approaches the 10^{-5}Å² range at 836 K, and starts to rise roughly around 3300 ps. The curve displays significantly more atomic motion and small local disorder, rising earlier and achieving the 10^{-4} Å² threshold by 905 K. The move from vibrational behaviour at low temperatures to observable diffusion at higher temperatures is supported by the increasingly steeper curves, as shown by **Figures 4 (a)**, **(b)**, and **(c)**.

3.4 Diffusion Coefficient from MSD Curve

To compute the diffusion coefficient of copper at the selected temperatures, the slope of the MSD vs. time curve is determined. The MSD approach is an effective technique to determine the diffusion coefficient of metals and alloys across various temperature ranges. As it increases the precision and consistency of the atomic movement (Gao et al., 2025). **Figure 5** depicts the linear fit curves of MSD vs. time at three selected temperatures. Least-squares linear regression is applied to precisely recognize and investigate the linear portion of these curves. The computed slope precisely describes atomic migration, because the chosen

portion coincides with the diffusive regime, where MSD rises linearly with time. In **Figures 5(a)**, **(b)**, and **(c)**, the chosen portion for linear regression is from 4300ps to 4800ps, 3700 ps to 4800ps, and 4000 ps to 4900ps, respectively. These selected time windows are also outside the ballistic region and provide a reliable value of diffusion coefficients. Multiple data points have been taken for the linear fit within the above-selected regions.

The statistical accuracy and uniform fitting behaviour are exhibited by the fitted parameters, such as the intercept and slope, which display little variation across the three temperatures. These small variations confirm that the above chosen fitting windows perfectly represent the underlying mechanism of the diffusion process with minimal numerical fluctuations.

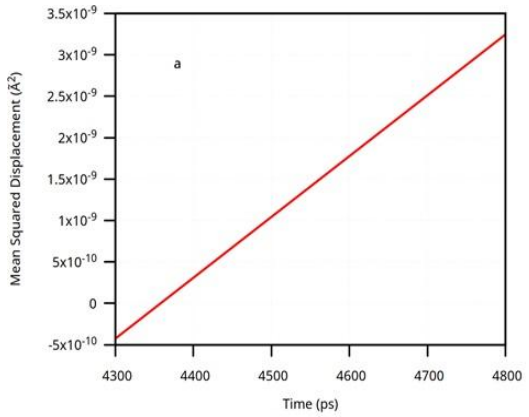

(a) 715 K

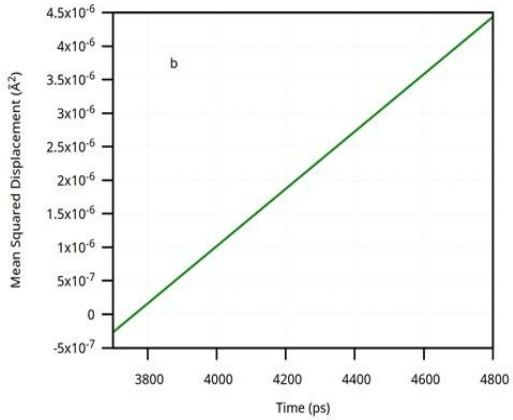

(b) 836 K

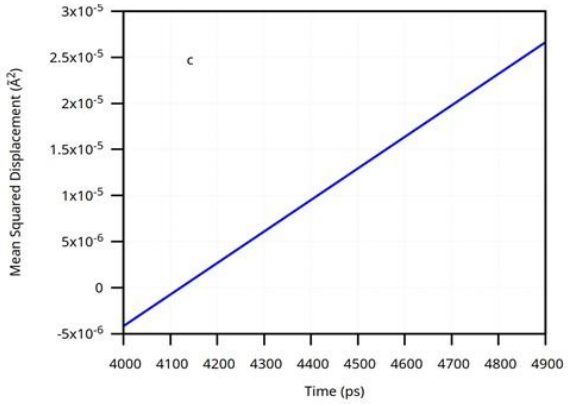

(c) 905 K

Figure 5. Linear fit curve of mean squared displacement vs time of copper metal at selected diffusive regime obtained at three selected temperatures (a) 715 K (b) 836 K (c) 905 K.

Table 3 gives the calculated and experimentally reported values of the copper diffusion coefficient at different temperatures, and it is clear that the thermally induced diffusion pattern is validated by the diffusion coefficients' persistent increase with temperature. This behaviour is associated with an Arrhenius-type relationship, in which atomic mobility and migration rates increase with temperature.

Table 3. Calculated and experimental value of diffusion coefficient of copper at the examined temperatures.

S. No.	Temperature(K)	D_{self} (cm^2/sec) calculated	D_{Self} (cm^2/sec) experimental	Reference
1.	715	$1.2x10^{-16}$	$4.8x10^{-16}$	Maier (1977)
2.	836	$7x10^{-14}$	$6.1x10^{-14}$	Maier (1977)
3.	905	$5.7x10^{-13}$	$6.2x10^{-13}$	Maier (1977)

Furthermore, it has been noticed from **Table 4** that the variation in the calculated and experimental values is high at low temperatures, but it reduces rapidly at higher temperatures, which implies better consistency at higher temperatures. At higher temperatures, this pattern can be justified by increased atomic mobility and diminished relative impact of simulation constraints.

Table 4. Absolute error between calculated and experimental values at three selected temperatures.

S. No.	Temperature (K)	D_{self}(cm^2/sec) calculated	D_{Self} (cm^2/sec) experimental	Absolute error
1.	715	$1.2x10^{-16}$	$4.8x10^{-16}$	3.6
2.	836	$7x10^{-14}$	$6.1x10^{-14}$	0.9
3.	905	$5.7x10^{-13}$	$6.2x10^{-13}$	0.6

The difference between the calculated and experimentally obtained values of the self-diffusion coefficient of copper arises due to various types of associated disparities between simulation conditions and real-world observations. Atomistic behavior can be affected by parameters that include the size of the simulation box, the total simulation time, and the imposed boundary conditions, that may lead to small departures from real experimental conditions. Also, a smaller simulation time frame cannot properly record slow migration rate or long-time equilibrium behavior, and a smaller simulation box can also hinder long-range atomic migrations. Additional changes may be generated by thermostat/barostat settings, finite-size effects, and the selection of the interatomic potential. Diffusion is determined in molecular dynamics under rigorously regulated and idealized settings where microstructural imperfections, impure substances, and grain boundaries have either been entirely removed or decreased. On the other hand, these defects frequently appear in experimental samples, which can roughly modify atomic mobility. Notwithstanding these variations, the calculated diffusion coefficient values indicate a distinct rising pattern with temperature, which is in accordance with the thermally stimulated behaviour of the diffusion, indicating that the simulation faithfully replicates experimentally verified patterns.

Figure 6 shows the OVITO visualization of the copper microstructure at the studied temperatures. These visualizations illustrate how temperature regulates the atomic displacement inside the simulation box. Although the diffusion begins at different times for each temperature, all three images have been captured at the same final simulation time to ensure a fair comparison. Consequently, the displacements are spread more widely and smoothly, with apparent green-yellow areas demonstrating moderate diffusion.

The atomic displacement magnitude with respect to the original reference configuration is illustrated by the color coding. A color gradient was employed, with red representing greater atomic displacement and blue denoting less displacement, whereas light green, yellow, and orange represent intermediate values. At 715 K, atoms only oscillate for a longer duration of time mainly because there is an insufficient amount of thermal energy to simulate early atomic jumping. Consequently, even at the final frame, the structure is largely blue-green, with only few small red regions exhibiting larger displacement, implying very sluggish and late diffusion. Since copper atoms possess a greater amount of kinetic energy at 836 K, hence they can depart their lattice sites earlier than at 715 K. By the final stage of the simulation, this leads to a more

refined and larger displacement distribution, with clear green-yellow and red zones showing noticeable moments of atoms. Due to the tremendous amount of thermal energy at 905 K, which allows atoms to quickly surmount the energy barriers, migration of atoms starts right after the simulation commences. Wide yellow and red zones are seen throughout the structure at 905 K, which indicates high, extensive atomic movement. These outcomes reveal that elevated temperatures not only enhance the rate of diffusion but also substantially expedite the start of diffusional motion, leading to greater atomic rearrangement as the temperature rises.

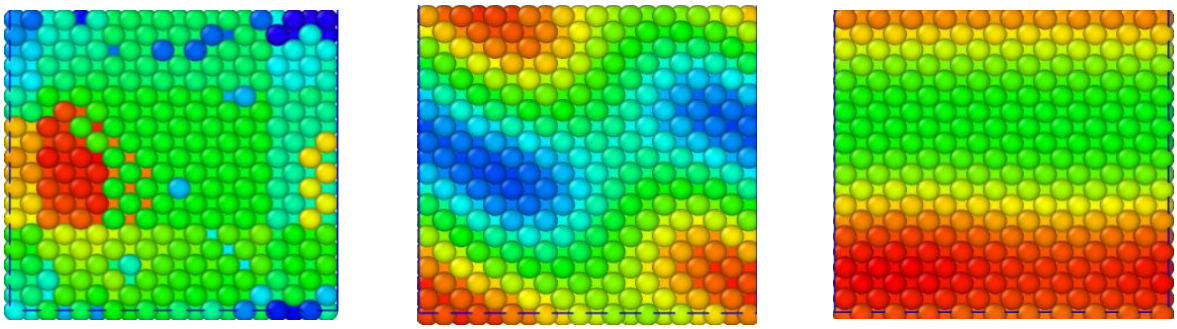

(a) 715 K (b) 836 K (c) 905 K

Figure 6. Microstructure evolution of copper metal at three selected temperatures (a) 715 K (b) 836 K (c) 905 K, showing atomic distribution and diffusive behaviour at the final simulation time.

4. Conclusion

This work successfully validates the use of molecular dynamics simulation as an efficient computational method for investigating the temperature-dependent self-diffusion attributes of copper at three selected temperatures. The work has systematically analysed the diffusion mechanisms via mean squared displacement calculations and radial distribution function analysis using the LAMMPS simulation package with the EAM potential. The output data of the LAMMPS simulation is used for the microstructural visualization with OVITO. The results further reveal a temperature-dependent progression in atomic mobility. As the temperature rises from lower to higher values, a significant increase in atomic migration is observed, implying a distinct self-diffusion regime. This temperature-activated increase in atomic displacement confirms the vacancy-mediated diffusion mechanism, a characteristic of FCC metals. The estimated self-diffusion coefficients give a satisfactory temperature-dependent pattern with reported experimental values. Whatever deviations are observed from the experimental results may be attributed to the computational limitations and the difference in microstructural imperfections, which are always present in real experimental samples. Structural analysis through radial distribution functions confirms that the FCC structure of copper remains stable across all investigated temperatures, despite increasing thermal vibrations. The preservation of distinct peaks up to 905 K indicates structural stability without phase transformation, though increased atomic mobility facilitates diffusion processes essential for material performance at elevated temperatures. The microstructure visualizations through OVITO provide a strong justification for the localized vibrations at 715 K to widespread atomic rearrangement at 905 K. These visualizations enhance the understanding of how thermal energy enables atoms to cross the energy barriers and contribute to the diffusive movement. To gain additional insight into copper migration under various thermodynamic parameters, further studies may include a larger number of intermediate temperatures.

Conflicts of Interest
There is no conflict of interest.

Acknowledgments
The authors express their sincere gratitude to PROF.(DR.) SUMITA SRIVASTAVA Principal Radhey Hari Government Post Graduate College, Kashipur (Kumaun University Nainital) for her valuable guidance, continuous encouragement, and insightful suggestions throughout this research work.

AI Disclosure
During the preparation of the present paper, we have used generative AI in order to improve the language of the present article. After using this tool, we have reviewed and edited the content as needed and take full responsibility for the content of the publication.

References

Barbhuiya, S., & Das, B.B. (2023). Molecular dynamics simulation in concrete research: a systematic review of techniques, models, and future directions. *Journal of Building Engineering, 76*, 107299. https://doi.org/10.1016/j.jobe.2023.107267

Butrymowicz, D.B., Manning, J.R., & Read, M.E. (1973). Diffusion in copper and copper alloys. part I. volume and surface self-diffusion in copper. *Journal of Physical and Chemical Reference Data, 2*(3), 643-655. https://doi.org/10.1063/1.3253129

Chui, C.P., Liu, W., Xu, Y., & Zhou, Y. (2015). Molecular dynamics simulation of iron - a review. *SPIN, 05*(04), 1540007. https://doi.org/10.1142/S201032471540007X

Gao, Y., Cao, X., & Zhong, Z. (2025). T-MSD: an improved method for ionic diffusion coefficient calculation from molecular dynamics. *Material Science.* arXiv preprint arXiv:2503.04281

Hargather, C.Z., & O'Connell, J.M. (2022). A systematic first-principles study of computational parameters affecting self-diffusion coefficients in FCC Ag, Cu, and Ni. *Journal of Phase Equilibria and Diffusion, 43*(6), 764-779. https://doi.org/10.1007/s11669-022-00991-4

Kuper, A., Letaw, H., Slifkin, L., Sonder, E., & Tomizuka, C.T. (1954). Self-diffusion in copper. *Physical Review, 96*(5), 1224-1229. https://doi.org/10.1103/physrev.96.1224

Kart, H.H., Yildirim, H., Ozdemir Kart, S.O., & Çağin, T. (2014). Physical properties of Cu nanoparticles: a molecular dynamics study. *Materials Chemistry and Physics, 147*(1-2), 204-212. https://doi.org/10.1016/j.matchemphys.2014.04.030

Li, C., Li, D., Tao, X., Chen, H., & Ouyang, Y. (2014). Molecular dynamics simulation of diffusion bonding of Al–Cu interface. *Modelling and Simulation in Materials Science and Engineering*, *22*(6), 065013. https://doi.org/10.1088/0965-0393/22/6/065013

Li, J., Wang, J., Li, X., & Qin, J. (2024). Composition-dependent diffusion and viscosity behavior in liquid Ti–Al–Ni ternary alloys. *Journal of Materials Research and Technology*, *33*, 3864-3873. https://doi.org/10.1016/j.jmrt.2024.10.086

Li, X.H., Ma, T., Chu, W.X., & Wang, Q.W. (2016). Molecular dynamics simulation on diffusion welding between Cu and Al under different pressures and roughnesses. In *Proceedings of the ASME 2016 14th International Conference on Nanochannels, Microchannels, and Minichannels* (V002T13A004). ASME. Washington, DC, USA. https://doi.org/10.1115/HT2016-7380

Mao, A., Zhang, J., Yao, S., Wang, A., Wang, W., Li, Y., Qiao, C., Xie, J., & Jia, Y. (2020). The diffusion behaviors at the Cu-Al solid–liquid interface: a molecular dynamics study. *Results in Physics*, *16*, 102998. https://doi.org/10.1016/j.rinp.2020.102998

Maier, K. (1977). Self-diffusion in copper at "low" temperatures. *Physica Status Solidi A*, *44*(2), 567-576. https://doi.org/10.1002/pssa.2210440220

Mishin, Y., Mehl, M.J., Papaconstantopoulos, D.A., Voter, A.F., & Kress, J.D. (2001). Structural stability and lattice defects in copper: *Ab initio,* tight-binding, and embedded-atom calculations. *Physical Review B*, *63*(22), 224106. https://doi.org/10.1103/PhysRevB.63.224106

Posselt, M., Bracht, H., Ghorbani-Asl, M., & Radić, D. (2022). Atomic mechanisms of self-diffusion in amorphous silicon. *AIP Advances*, *12*(11), 115325. https://doi.org/10.1063/5.0111037

Riahi, M.K., Qattan, I.A., Hassan, J., & Homouz, D. (2019). Identifying short- and long-time modes of the mean-square displacement: an improved nonlinear fitting approach. *AIP Advances*, *9*(5), 055112. https://doi.org/10.1063/1.5098051

Rothman, S.J., & Peterson, N.L. (1969). Isotope effect and divacancies for self-diffusion in copper. *Physica Status Solidi* (*b*), *35*(1), 305-312. https://doi.org/10.1002/pssb.19690350131

Singh, N.S.S., Hassan, W.H., Thiab, R.F., Al-zahy, Y.M.A., Salahshour, S., & Hekmatifar, M. (2025). Effect of copper nanoparticle volume fraction on flow in a 3D lid-driven cavity with phase change materials using molecular dynamics simulation. *Case Studies in Chemical and Environmental Engineering*, *11*(3), 101181. https://doi.org/10.1016/j.cscee.2025.101181

Steigman, J., Shockley, W., & Nix, F.C. (1939). The self-diffusion of copper. *Physical Review*, *56*(1), 13-21. https://doi.org/10.1103/PhysRev.56.13

Trong, D.N., Long, V.C., & Tălu, Ş. (2022). Molecular dynamics simulation of bulk Cu material under various factors. *Applied Sciences, 12*(9), 4437. https://doi.org/10.3390/app12094437

Tatsumi, H., Kao, C.R., & Nishikawa, H. (2023). Impact of crystalline orientation on Cu–Cu solid-state bonding behavior by molecular dynamics simulations. *Scientific Reports*, *13*(1), 23030. https://doi.org/10.1038/s41598-023-50427-3

Talanin, V.I., & Talanin, I.E. (2016). Diffusion model of the formation of growth microdefects: a new approach to defect formation in crystals (review). *Physics of the Solid State*, *58*(3), 427-437. https://doi.org/10.1134/S106378341603029X

Wade, A.D., Wang, L.-P., & Huggins, D.J. (2018). Assimilating radial distribution functions to build water models with improved structural properties. *Journal of Chemical Information and Modeling*, *58*(9), 1766-1778. https://doi.org/10.1021/acs.jcim.8b00166

Yang, J., Zhang, J., & Qiao, J. (2019). Molecular dynamics simulations of atomic diffusion during the Al–Cu ultrasonic welding process. *Materials, 12*(14), 2306. https://doi.org/10.3390/ma12142306

Yang, L., Zhang, Y., & Chen, J.K. (2011). Molecular dynamics simulation of deposition of nickel nanocluster on copper surface. *Journal of Nanoparticle Research*, *13*(10), 4479-4489. https://doi.org/10.1007/s11051-011-0400-5

Yin, T., Wang, G., Guo, Z., Pan, Y., Song, J., Ding, Q., & Zhao, G. (2024). Molecular dynamics simulation on polymer tribology: a review. *Lubricants, 12*(6), 205. https://doi.org/10.3390/lubricants12060205

Ye, Z.H., Liu, J.H., Chai, C.G., Wen, Y.-S., Cui, S.-X., Zhang, G.-Q., Li, K.-J., Guo, F., & Wang, X.-C. (2025). ReaxFF-nn: a reactive machine-learning potential in GULP/LAMMPS and its applications in the thermal conductivity calculations of carbon nanostructures. *Physical Chemistry Chemical Physics*, *27*(20), 10571-10579. http://dx.doi.org/10.1039/D4CP00535J

Zhang, C., Shomali, A., Coasne, B., Derome, D., & Carmeliet, J. (2023). Sorption–deformation–percolation model for diffusion in nanoporous media. *ACS Nano*, *17*(15), 10084-10094. https://doi.org/10.1021/acsnano.2c10384

Zhang, S., Ma, T., Zhao, Y., Zhang, Z., Shao, W., Huang, J., Zhang, X., Ye, Z., Wang, W., & Yang, J. (2024). Microstructure and mechanical properties of copper/Al interlayer/graphite joint prepared utilizing "two-stage method" vacuum diffusion bonding. *Vacuum*, *227*, 113414. https://doi.org/10.1016/j.vacuum.2024.113414